



# Kinetics, Isotherm and Thermodynamic Properties of the Basement Complex of Clay Deposit in Ire-Ekiti Southwestern Nigeria for Heavy Metals Removal

S. S. Asaolu, S. O. Adefemi, O.A. Ibigbami†, D.K. Adekeye and S. A. Olagboye

Department of Chemistry, Ekiti State University, Ado-Ekiti, Nigeria

†Corresponding author: Ibigbami O.A.; olayinkaibigbami@yahoo.co.uk

Nat. Env. & Poll. Tech.  
Website: [www.neptjournal.com](http://www.neptjournal.com)

Received: 10-06-2019  
Revised: 29-06-2019  
Accepted: 30-08-2019

## Key Words:

Adsorption  
Heavy metal removal  
Kinetic isotherms  
Kaolinite  
Ire-Ekiti

## ABSTRACT

Raw kaolinite clay collected from Ire-Ekiti, Ekiti State, Nigeria, was used to adsorb some heavy metals (Pb, Cr, Ni and Cu) from their aqueous solution through batch experiments. Adsorption studies were performed at the different temperatures, concentration and time to determine the kinetics, isotherm and thermodynamic properties of the adsorption processes. The adsorption thermodynamic properties showed that sorption of Cu, Cr and Ni on the raw clay was exothermic, while adsorption of Pb was endothermic. The negative values of  $\Delta G$  for Pb adsorption revealed the feasibility and spontaneity of the adsorption process while the positive  $\Delta G$  values for Cu, Cr and Ni sorption showed non-spontaneity of the adsorption process. Langmuir, Freundlich and Elovich isotherms were applied to explicate the nature of adsorption process, while Pseudo-first-order (PFO), Pseudo-second-order and Elovich kinetics were applied to literarily determine the adsorbate-adsorbent interaction. Pseudo-second-order kinetics was the best fitting kinetics for adsorption of the metals on the raw clay.

## INTRODUCTION

The presence of heavy metals like chromium, copper, lead, nickel, arsenic, etc. in water bodies, has become a growing environmental problem. Water bodies are mostly contaminated with these heavy metals through anthropogenic activities. These heavy metals enter into water bodies through various industrial processes, including metal plating, fertilizer production, mining, metallurgy, battery manufacturing and textile dyeing, and others (Barhoumi et al. 2009, Eloussaief & Benzina 2010). Their potential toxicity, persistence and bio-accumulation problems pose a great threat to both man and other forms of life. High concentrations of them in the environment may constitute long-term health risks to ecosystems and humans.

A wide range of various treatment techniques such as ion exchange, photodegradation, biosorption, oxidation, electrochemical treatment, precipitation, and adsorption have been reportedly used for removal of heavy metal ions from industrial effluents (Bailey et al. 1999, Ku & Jung 2001, Babel & Kurniawan 2003, Bradl 2004, Fu & Wang 2011, Shim et al. 2014). However, adsorption has been universally accepted as one of the most effective pollutant removal processes, with low cost, ease in handling, low consumption of reagents, as well as scope for recovery of value-added components through desorption and regeneration of adsorbent (Olivella et al. 2011, Dawodu et al. 2012). Materials that have been used as an adsorbent for heavy metals include rubber seed

coat pecan shells, jute fibre (Senthilkumaar et al. 2005), Indian rosewood sawdust, olive stones, pinewood and clay (Rengaraj et al. 2002, Shawabke et al. 2002, Tsenga et al. 2003, El-Sheikh et al. 2004, Garg et al. 2004).

Clay plays an important role in the environment by acting as a natural pollutant remover, taking up cations and anions either through ion exchange, surface complexation, pore diffusion, precipitation or direct bonding (Arnamwong et al. 2016, Emam et al. 2016). Natural clays have been known to possess a reasonable ability to remove heavy metal contaminants from their contaminated medium. Clays from Africa have been reportedly used for the removal of heavy metals and they have been found to possess great removal efficiency for the metals (Eloussaief et al. 2009, Mbaye et al. 2014, Olu-owolabi et al. 2016, Adekeye et al. 2019). A recent study by Adekeye et al. (2019) has reported the adsorption properties of Cu, Ni, Pb and Cr of the basement complex of clay deposit from the present study area. The present work is aimed at elucidating the kinetics, isotherm and thermodynamics properties of the adsorption processes of the metals on the clay adsorbent.

## MATERIALS AND METHODS

### Sample Collection and Preparation

The clay soil was collected from Ire-Ekiti, Southwestern Nigeria. Both topsoil (at the depth of 5 cm away from the

surface) and subsurface soil (at the depth of 15 cm away from the surface) were taken at four cardinal points with equidistance of 0.5 km away from one another. The soil samples were homogeneously mixed to obtain a representative sample for use. An adequate amount of the sample for use was taken, dried at room temperature, crushed and dispersed in deionized water. Floating debris from plants was removed by handpicking and also by decantation. The suspension was thoroughly stirred to separate non-clay materials from the clay. The clay soil was recovered from the water by centrifuging the suspension at 3000 rpm. The recovered clay soil was oven-dried at 110°C for 12 hours and cooled in a desiccator. After cooling, the dried clay sample was crushed in a ceramic mortar and sieved through sieves of different sizes ranging from 200-500 µm. The sieved clay soil was stored in a black polyethylene bags prior to subsequent analysis.

### Preparation of Metal Solution

The reagents used to prepare solutions of metal ions were of analytical grades. The stock solutions (1000 mg.L<sup>-1</sup>) of the metal ions (Ni, Pb, Cu and Cr) were prepared by dissolving weighed quantities of metal salts (potassium chromate, lead nitrate, copper nitrate and hydrated nickel sulphate) in deionised water and serially diluted to prepare solutions of varying initial concentration for as required for the experimental works. Both the initial and equilibrium concentrations of metal ions were determined using an Atomic Absorption Spectrophotometer (Agilent AAS 55AA).

### Characterization

The functional group determination of the clay soil was carried out by Fourier Transformed Infrared Spectrophotometer (FTIR). Scanning Electron Microscope (SEM) was used to show surface morphology of the clay soil while the elemental composition was determined by Energy Dispersive X-ray Emission technique.

### Batch Adsorption Experiments

Adsorption experiments were carried out in batch by adding 50 mL of 10 mg/L adsorbate solution into conical flasks containing 0.50 g of the adsorbent. The adsorbent and adsorbate mixtures were then equilibrated at pH value of 5.0 by shaking at 200 rpm in temperature (298 K) using a rotary orbital shaker until equilibrium. After equilibration, the mixtures were centrifuged for 10min at 3000 rpm after which the supernatants were collected and analysed for equilibrium concentrations of the Cu, Ni, Pb and Cr using AAS. To study the adsorption isotherm, adsorption of Cu, Ni, Pb and Cr onto the clay soil was optimized at different concentrations of 20, 40, 60, 80 and 100 ppm with an equilibration time of 90 min at pH value of 5. Agitation time was varied from 10 to 80 min also at pH 5 to study the adsorption kinetics. The adsorption temperatures of 300, 315, 330, 340 and 350 K were implored to understand the thermodynamic properties of the adsorption process.

## RESULTS AND DISCUSSION

### Morphology of the Raw Clay Soil

The SEM image (Fig. 1) of the raw clay soil showed a dense arrangement of the particles. This arrangement results from the stacking of the particles upon one another. Inter-aggregate pores which could allow permeation of adsorbates on the clay soil are also present in small size.

### Elemental Composition of the Raw Clay Soil

The result from Energy Dispersive X-ray Emission technique (Fig. 2) showed that oxygen, aluminium and silicon are the major elemental constituents and possessing the highest percentage by weight (20.70, 15.10 and 50.00 respectively) of the raw clay soil. The presence of oxygen and the absence of hydrogen showed that the elements were present in the form of oxide rather hydroxide. The elemental composition

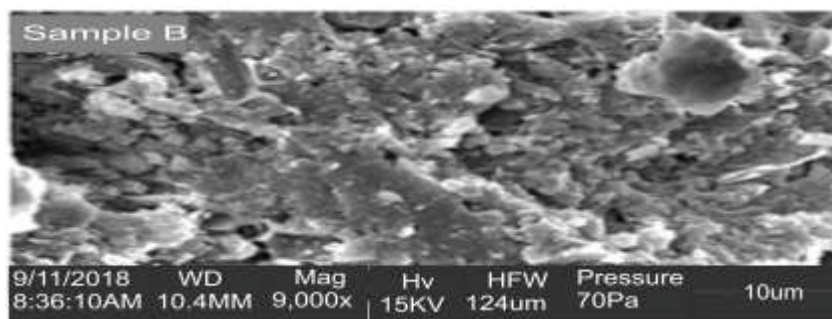


Fig. 1: SEM image of the raw clay soil.

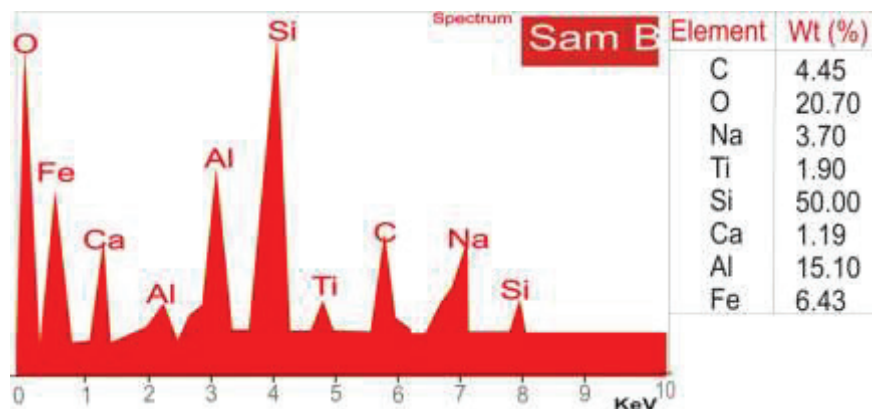


Fig. 2: EDX spectra of the raw clay soil

of the raw clay soil also showed that the clay soils contained some important exchangeable cations such as Na (3.70 %), Ca (1.19 %) and Fe (6.43 %). The presence of these exchangeable cations in the soil could bring about the ion-exchange mechanism for the removal of the adsorbates from their respective solution. The percentage abundance by weight of Si and Al compared to other elements showed that the clay soil is kaolinite.

#### Fourier Transform Infrared Spectra of the Raw Clay Soil

The bands at 1633 and 1402  $\text{cm}^{-1}$  (Table 1) are due to the

presence of C=O and C=C which indicate the presence of organic matter in the clay soil. The band at 536  $\text{cm}^{-1}$  is due to the presence of Si-O-Al group. The absorption bands at 3671 and 3620  $\text{cm}^{-1}$  showed the presence of OH group of bonded water while the bands at 3421 and 3263  $\text{cm}^{-1}$  showed the OH group of organic matter and also confirming the presence of organic matter in the clay soil.

The presence of metallic oxide in the clay soil is shown by the intensity bands at 468 and 432  $\text{cm}^{-1}$ . The FTIR result (Fig. 3) of this study is consistent to the results of Van der-Marel & Beutelspacher (1976), Petit et al. (1995), Wilson (1994) and Saikia et al. (2003) on the characterization of clay minerals.

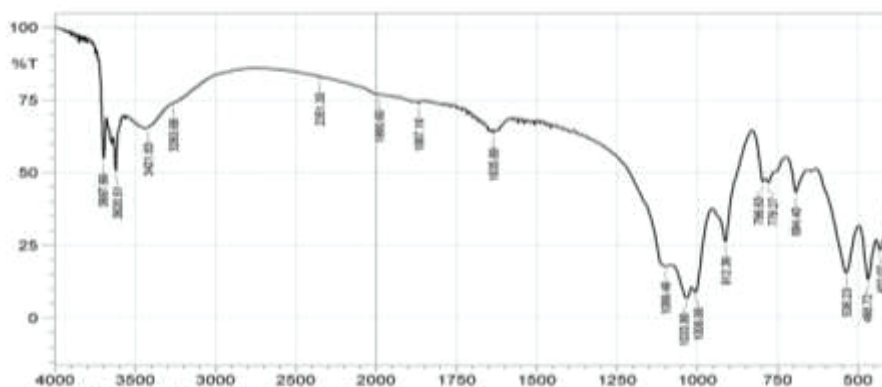


Fig. 3: Fourier Transform Infrared Spectra of the raw clay soil.

Table 1: Fourier Transform Infrared spectra of the raw clay soil

M-O	OH	C=C	C=O	Si-O-Si	Si-O-Al
468, 432	3671, 3620 3421, 3263	1420	1633	1099-1006	536

## Effect of Adsorption Parameters

**Effect of agitation time:** The effect of agitation time on the removal of Ni, Pb, Cu and Cr is shown in Fig. 4. The removal of Pb by the raw clay was optimized (98.75%) within a short period (40 min) and tended to be stable for 80 min. The optimum removal of copper was observed to be at 60 min then tended to be stable after 60 min while Cr and Ni adsorption increased with increase in time until equilibration was achieved at 60 and 70 min for the metals respectively. The increased adsorption during the initial stages might be due to the presence of abundant active sites on the surface of the clay soil, which became saturated with time until equilibrium was attained.

A good adsorbent does not only have high adsorption efficiency but also a fast rate of adsorption (Akpomie et al. 2017). It could also be seen that the equilibrium adsorption time for all the metals was attained within 30-70 min. This showed that the clay soil is good enough to be applied for both domestic and industrial purposes for the removal of heavy metals from contaminated aqueous medium.

## Effect of Adsorbate Concentrations

The concentration of adsorbates is also an important parameter in an effective adsorption study. The effect of adsorbate concentration on adsorption process on the raw clay soil is shown in Fig. 5. Results from this study showed that the adsorption capacity of raw clay soil increased with increase in metal ion concentration from 20 mg/L to 100 mg/L.

This trend was attributed to the fact that when the transport of metals between the adsorbent's external surface film and internal pores are equal, the trans-boundary movement of metals will not be significantly permissible; however, increasing concentration could re-initiate the trans-boundary movement (depending on the nature of the adsorbate and adsorbent) and hence, the adsorption process would be concentration dependent. Similar results were also reported by Eba (2010), Mbaye et al. (2014) and Zourabi (2016).

## Effect of Temperature

The temperature has been shown to possess significant effects on adsorption phenomenon (Zourabi et al. 2016,

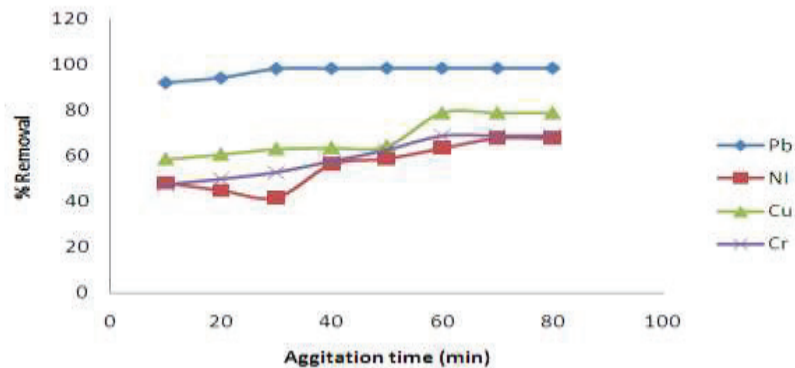


Fig. 4: Adsorption trend with increase agitation time.

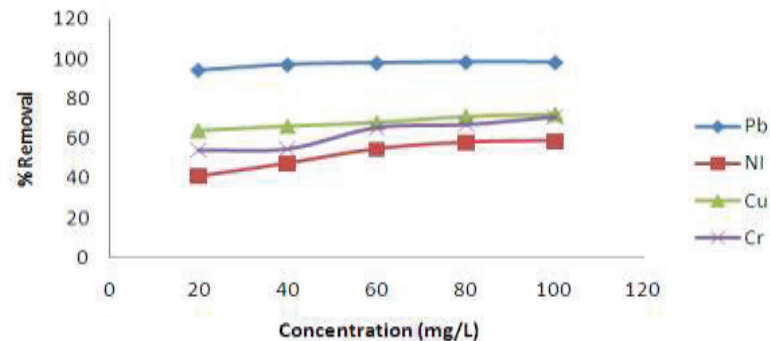


Fig. 5: Adsorption trend with increase in concentration.

Akpomie et al. 2017). Temperature affects two major aspects of adsorption *viz* the equilibrium position in relation with the exothermicity and endothermicity of the process and the swelling capacity of the adsorbent (Rattanaphani et al. 2007, Natalia et al. 2015). Thus, adjustment of temperature may be required in the adsorption process. As observed in the raw clay soil (Fig. 6), the uptake capacity of Pb decreased with increasing temperature.

This is due to the endothermic effect of the surroundings during the adsorption process while the adsorption of Ni, Cu and Cr by the raw clay soil increased with temperature increase. This showed the potential of copper, chromium and nickel to overcome resistance to mass transfer with increase kinetic energy to undergo an interaction with the active sites of the adsorbents. Similar results to this study have been reported by Gonzalez et al. (2005), Rattanaphani et al. (2007), El-Sayed et al. (2011) and Zourabi et al. (2016).

### Adsorption Kinetics

**Pseudo-first-order kinetics:** The adsorption data were modelled using the Lagergren pseudo-first-order model given by:

$$\log (q_e - q_t) = -\frac{k_1}{2.303}t + \log q_e \quad \dots(1)$$

This model was used to predict physical adsorption mechanism for the metals' adsorption processes on the raw clay. Where  $q_t$  (mg/g.min) is the amount of metal adsorbed on the surface of the sorbent at time  $t$  (min),  $q_{e, \text{is}}$  the amount of metal adsorbed at equilibrium and  $K_1$  ( $\text{min}^{-1}$ ) is the equilibrium rate constant of pseudo-first-order adsorption (Lagergren 1908). The rate constant  $K_1$ , was calculated from the slope of  $\log (q_e - q_t)$  versus time  $t$  for plots in which straight lines were obtained. If a straight line is obtained and  $q_{e, \text{Cal}}$  values are close to  $q_{e, \text{Exp}}$  it suggests the applicability of the model.

Results of this research showed that straight line graphs were obtained for metals adsorption on the raw clay soil as shown in Fig. 7.

But the values of  $q_{e, \text{Cal}}$  did not correlate to those of  $q_{e, \text{Exp}}$  as given in Table 2 which suggests that the adsorption processes cannot be represented by pseudo-first-order kinetics model.

**Pseudo-second-order kinetics:** The linearized pseudo-second-order kinetics was also applied to evaluate its applicability.

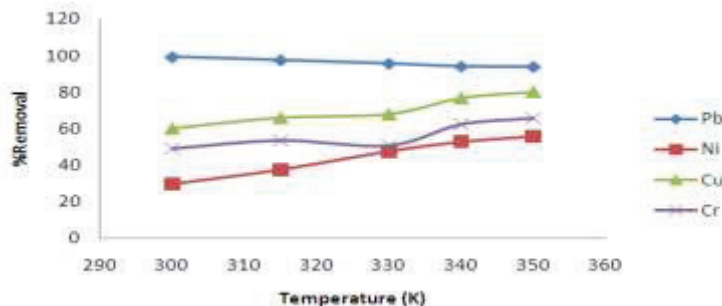


Fig. 6: Adsorption trend with increase in temperature for the metals.

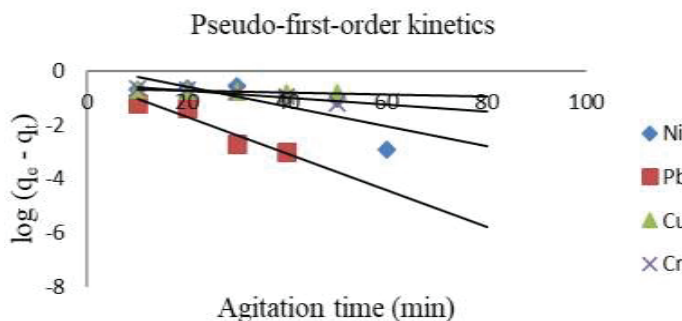


Fig. 7: Plot of  $\log (q_e - q_t)$  vs agitation time (min) for raw clay.



Table 2: Pseudo first-order kinetics for raw clay

	Pb	Ni	Cu	Cr
$R^2$	0.9033	0.5736	0.9330	0.9078
$K_I$	1.566	0.0836	0.0083	0.0299
$q_{eExp}$	0.4193	1.3424	0.2125	0.3334
$q_{eCal}$	0.988	0.680	0.790	0.699

Table 3: Pseudo-second-order kinetics for raw clay

	Pb	Ni	Cu	Cr
$R^2$	0.9999	0.9463	0.9712	0.9837
$K$	1.242	0.1117	0.1478	0.1467
$q_{eExp}$	1.009	0.7968	0.866	0.7833
$q_{eCal}$	0.988	0.680	0.790	0.699

It is given by equation (2):

$$\frac{t}{q_t} = \frac{1}{h} + \frac{t}{q_e} \quad \dots(2)$$

Where,  $h = k_2 q_e^2$  [mg/(g.min)].

Hence, the pseudo-second-order equation can be written as:

$$\frac{t}{q_t} = \frac{1}{k_2 q_e^2} + \frac{t}{q_e} \quad \dots(3)$$

Where,  $qt$  (mg/g.min) is the amount of metal adsorbed on the surface of the sorbent at time  $t$ ,  $k$  (g/(mg.min)) is the pseudo-second-order rate constant, while  $q_e$  (mg/g) is the amount of metal adsorbed at equilibrium. The values of  $q_e$ ,  $k$  and  $h$  were determined experimentally by plotting  $1/q_t$  against  $t$ .

Pseudo-second-order plots for the raw clay are shown in Fig. 8, the values of  $q_{eCal}$  for the sorption process of all the metal adsorbates onto the raw clay correlate to those of  $q_{eExp}$  as given in Table 3. This shows that the adsorption process can be represented by pseudo-second-order kinetics. The  $R^2$  values of the pseudo-second-order for all the metals' adsorption processes are closer to unity than the pseudo-first-order plot. This showed that the sorption processes best fit the pseudo-second-order kinetics.

The fitting of the adsorption processes to pseudo-second-order kinetics implies that there is a possible chemical interaction between the adsorbates and adsorbent during sorption processes. It could also be assumed that the rate-limiting step may be chemical sorption involving valence forces, through exchange or sharing of electrons between sorbate and sorbent. Similar results of this study were observed in studies conducted by Ho & Mckay (1999) and Nethaji et al. (2013).

**Elovich kinetics:** The Elovich kinetics was modelled us-

ing the linear form of the equation as represented in equation (4) (Kumara et al. 2011).

$$q_t = \frac{1}{\beta} \ln(\alpha\beta) + \frac{1}{\beta} \ln(t) \quad \dots(4)$$

The constants  $\alpha$  and  $\beta$  could be obtained from the slope and intercept of the linear plot of  $qt$  versus  $\ln t$ . Table 4 gives the Elovich kinetic parameters and Fig. 9 shows Elovich kinetic plots.

The correlation coefficient values (Fig. 9) for all the metals adsorption processes are less close to unity than the pseudo-first-order and pseudo-second-order kinetics. This suggests that the adsorption processes cannot be represented by the Elovich model.

### Adsorption Isotherms

The adsorption isotherms were used to show the sorption processes of the metals on the raw clay. This was achieved through the imploration of Langmuir, Freundlich, and Elovich plots.

**Langmuir adsorption isotherm:** The linearized Langmuir equation was used to show the surface binding properties of Cr. This was done using equation (5) (Kinnburgh 1986):

$$\frac{1}{q_e} = \frac{1}{Q_0} + \frac{1}{Q_0 K_L C_e} \quad \dots(5)$$

Where,  $C_e$  (mg/L) is the equilibrium concentration,  $q_e$  (mg/g) is the amount of ion adsorbed,  $Q_0$  ( $q_{max}$ ) maximum monolayer coverage capacity (mg/g) and  $K_L$  (L/mg) is Langmuir adsorption equilibrium constant. The values of  $q_{max}$  and  $K_L$  were computed from the slope and intercept of the Langmuir plot of  $1/q_e$  versus  $1/C_e$  (Langmuir 1918). The essential features of the Langmuir isotherm were also expressed in terms of equilibrium parameter  $R_L$ , which is a

dimensionless constant, referred to as separation factor or equilibrium parameter.

$$R_L = \frac{1}{1 + (K_L C_o)} \quad \dots(6)$$

Where,  $C_o$  is the initial concentration and  $K_L$  is the constant related to the energy of adsorption. If  $K_L$  is less than ( $<$ ) 0 the adsorption process does not correlate to Langmuir isotherm. Separation factor  $R_L$  value indicates the adsorption nature to be either unfavourable if  $R_L$  greater than ( $>$ ) 1, linear if  $R_L = 1$ , favourable if  $0 < R_L < 1$  and irreversible if  $R_L = 0$ . A negative  $R_L$  value indicates that the adsorption process does not fit Langmuir isotherm, hence, cannot be explained using the Langmuir isotherm.

From the data calculated in Table 5, the  $K_L$  and  $R_L$  values for Ni, Pb and Cu adsorption on the raw clay are  $< 0$  which showed that the adsorption processes could not be explained by Langmuir isotherm. On the other, the  $K_L$  value for Cr on the raw clay was 54.34 L/mg. Also,  $R_L$  values in the range of  $1.84 \times 10^{-5}$  and  $9.2 \times 10^{-4}$  were also obtained for the raw clay. The  $R_L$  values for chromium adsorption on the raw clay is greater than 0 but less than 1, thus, Langmuir isotherm is favourable; the positive  $K_L$  values are indicative that the adsorption processes correlate to the Langmuir isotherm. The  $R^2$  values for Cr, Pb, Cu and Ni adsorption onto the raw clay are 0.9837, 0.7531, 0.9705 and 0.9937 respectively. Even though Ni has the highest  $R^2$  value (0.9937), but its negative  $K_L$  value (-56.81) showed that its adsorption does

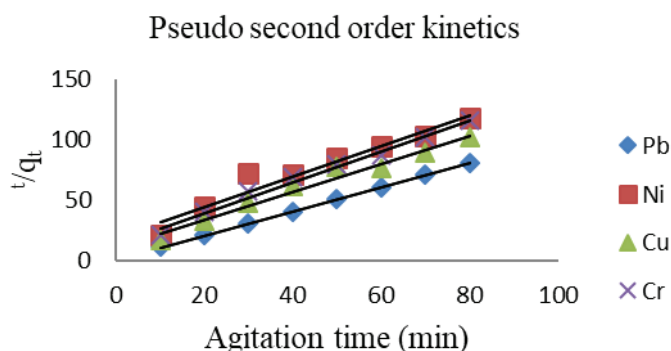


Fig. 8: Plot of  $1/q_t$  vs agitation time (min) for the raw clay.

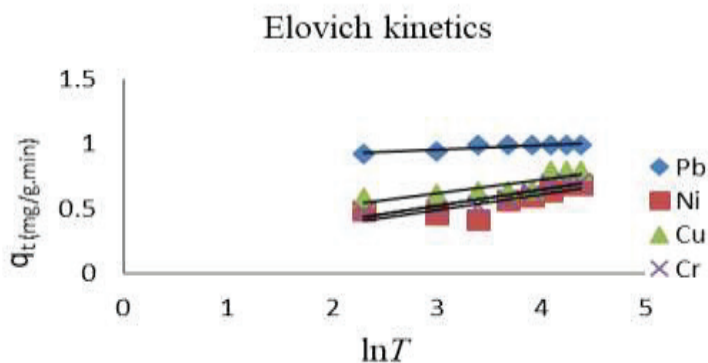


Fig. 9: Plot of  $q_t$ (mg/g.min) vs  $\ln T$  for the raw clay.

Table 4: Elovich kinetics parameters for the raw clay

	Pb	Ni	Cu	Cr
$R^2$	0.8565	0.6696	0.7159	0.8929

Table 5: Langmuir isotherm parameters for raw clay

	Ni	Pb	Cu	Cr
$R^2$	0.9937	0.7531	0.9705	0.9837
$q_{max}$	0.0578	0.1800	0.162	-0.0978
$K_L$	-56.81	-11.90	-59.88	54.34
$R_L$	$-(2 \times 10^{-4} - 9 \times 10^{-4})$	$-(8 \times 10^{-4} - 4.2 \times 10^{-3})$	$-(1.7 \times 10^{-4} - 8.4 \times 10^{-4})$	$(1.84 \times 10^{-5} - 9.2 \times 10^{-4})$

not correlate to the Langmuir isotherm.

This shows that  $R^2$  value is not sufficient to show the fitness of an adsorption process to Langmuir isotherm. The data obtained from the isotherms showed that chromium adsorption on the raw clay is in best compliance with the Langmuir isotherm. This implies monolayer adsorption of Cr on the clay's flat surfaces. The correlation was not only judged by the linear regression coefficient but also other parameters of the tested isotherms as the  $R^2$  value is not enough to describe the fitness and correlation of an adsorption process to Langmuir isotherm.

**Freundlich isotherm:** Freundlich isotherm was used to show possible multilayer adsorption process of Ni and Cu on the clay's rough surfaces. The Freundlich isotherm was elucidated using equation (7) and (8) (Freundlich 1906).

$$q_e = K_F C_e^{1/n} \quad \dots(7)$$

Where  $K_F$  is Freundlich isotherm constant (mg/g),  $n$  is adsorption intensity, and  $C_e$  is the equilibrium concentration of adsorbate (mg/L). Hence,

$$\log q_e = \log K_F + \frac{1}{n} \log C_e \quad \dots(8)$$

$K_F$  and  $1/n$  are empirical constants, indicating the adsorption capacity and the strength of adsorption in the adsorption process respectively.  $K_F$  and  $1/n$  were obtained by plotting  $\log q_e$  against  $\log C_e$  (Voudrias et al. 2002). If the value of  $1/n$  is below one it indicates normal adsorption. On the other hand, if  $1/n$  is above one, it indicates cooperative adsorption (Mohan & Karthikeyan 1997). Linear regression is generally used to determine the parameters for the Freundlich isotherm model (Guadalupe et al. 2008).

From the data in Table 6, the values of  $1/n$  are greater than 1 for Cr, Pb and Cu sorption processes onto the raw clay soil. This showed that the adsorption processes were cooperative while the sorption of Ni on the raw clay was favourable. From all the isotherms, the highest  $R^2$  values for Cu (0.9663) and Ni (0.9287) were obtained from the Freundlich isotherm. This shows that the adsorption processes of the Cu and Ni on the raw clay fit best to the Freundlich isotherm than other adsorption isotherms.

Thus, the adsorption process of Ni and Cu describes a heterogeneous system characterized by multilayer adsorption on the rough surfaces of the clay. A similar result in this study was also reported by Olu-owolabi et al. (2016).

**Elovich isotherm:** Elovich isotherm was used to show the multilayer adsorption of Pb on the raw clay.

The isotherm was modelled using equation (9), as expressed by Achmed et al. (2012):

$$\frac{q_e}{q_m} = K_e C_e e^{-\frac{q_e}{q_m}} = \quad \dots(9)$$

The linear regression coefficient was used to judge the correlation. The regression coefficient for Pb sorption on the raw clay is 0.9344 which is higher than that for Langmuir and Freundlich isotherms as given in Table 7.

Therefore, the adsorption of Pb on the raw clay does fit the Elovich isotherm better than others. This implies that Pb adsorption on the raw clay is based on a kinetic principle which assumes that adsorption sites increase exponentially with adsorption; thus, Pb sorption is multilayer adsorption.

Table 6: Freundlich isotherm parameters for the raw clay

	Cu	Ni	Cr	Pb
$R^2$	0.9963	0.9287	0.9502	0.8375
$K_f$	1.20	0.787	0.029	1.27
$n$	0.817	6.211	0.625	0.080
$1/n$	1.228	0.161	1.599	12.39



### Adsorption Thermodynamics

The adsorption thermodynamics was used to elucidate the nature of adsorption. Thermodynamic parameters associated with adsorption which include equilibrium constant  $K$ , that depends on temperature, the change in free energy  $\Delta G$  (KJ/mol), enthalpy  $\Delta H$  (KJ/mol) and entropy  $\Delta S$  (J/mole.K) associated to the adsorption process were calculated by following equations (Ramesh et al. 2005).

The free energy ( $\Delta G$ ) of the adsorption process is given by equation (10)

$$\Delta G = \Delta H - T\Delta S \quad \dots(10)$$

By considering the adsorption equilibrium constant  $K$ , the equation could be written as:

$$\Delta G = -RT \ln K \quad \dots(11)$$

$T$  is the temperature in Kelvin and  $R$  is gas constant ( $8.314 \text{ J mol}^{-1} \text{ K}^{-1}$ ).

$$K = \frac{q_e}{C_e} \quad \dots(12)$$

$$\ln K = \ln \frac{q_e}{C_e} \quad \dots(13)$$

Hence,  $\Delta H$  and  $\Delta S$  were calculated from the slope and intercept of the plot of  $\ln K$  vs  $1/T$  (Fig. 10).

The sorption of Pb on the raw clay decreased with increase in temperature as given Table 8. This is because an increase in temperature results to increase in entropy of the system.

The positive values of  $\Delta S$  for Pb sorption on the raw clay reflects an increased degree of disorderliness at the solid-liquid interface during the adsorption of Pb on the raw clay. On the other hand, the values of  $\Delta S$  for sorption of Cu, Cr and

Table 7: Elovich isotherm parameters for the raw clay

	Pb	Ni	Cu	Cr
$R^2$	0.9344	0.6186	0.2548	0.7093

Table 8: Thermodynamic parameters for the raw clay.

	Temp.	$1/T$	$C_e$	$q_e$	$\frac{q_e}{C_e}$	$\ln \frac{q_e}{C_e}$	$\Delta G$	$\Delta H$	$\Delta S$
Pb	300	0.00333	0.068	0.993	14.60	2.618	-6686.95		
	315	0.00317	0.245	0.976	3.984	1.382	-3477		
	330	0.00303	0.514	0.949	1.846	0.613	-1681.84	11.93	7898.14
	340	0.00294	0.586	0.941	1.606	0.474	-1339.88		
	350	0.00286	0.614	0.939	1.529	0.425	-1236.71		
Ni	300	0.00333	6.999	0.300	0.043	-3.147	7849.25		
	315	0.00317	6.216	0.378	0.061	-2.797	7325.09		
	330	0.00303	5.223	0.478	0.092	-2.386	6546.28	-129.40	-57402.71
	340	0.00294	4.711	0.529	0.112	-2.189	6187.78		
	350	0.00286	3.416	0.558	0.192	-1.650	4801.34		
Cu	300	0.00333	3.993	0.601	0.151	-1.890	4714.04		
	315	0.00317	3.411	0.659	0.193	-1.645	4308.11		
	330	0.00303	3.214	0.679	0.211	-1.556	4269.07	-92.23	-38973.72
	340	0.00294	2.330	0.767	0.329	-1.112	3143.36		
	350	0.00286	1.998	0.800	0.400	-0.916	2665.47		
Cr	300	0.00333	5.080	0.492	0.097	-2.333	5818.97		
	315	0.00317	4.627	0.537	0.116	-2.154	5641.13		
	330	0.00303	4.220	0.509	0.137	-1.988	5454.32	-48.75	-28250.36
	340	0.00294	3.732	0.627	0.168	-1.784	5042.74		
	350	0.00286	3.393	0.661	0.195	-1.635	4757.69		

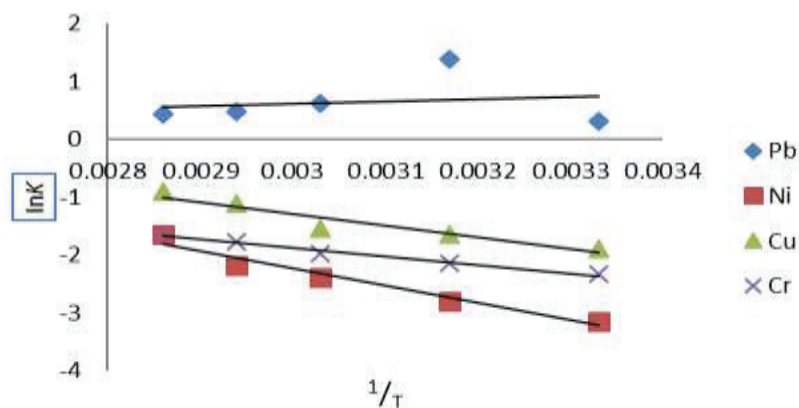


Fig. 10: plot of  $\ln K$  against  $1/T$  for the raw clay.

Ni were negative, which implies a decrease in randomness at the solid-solution interface during sorption of the metals on the raw clay adsorption; hence, the adsorption was favoured with the increase in temperature. The endothermic nature of Pb sorption by the raw clay was confirmed by the positive values of  $\Delta H$ , while the negative  $\Delta H$  values for Cu, Cr and Ni sorption showed exothermicity of the adsorption processes.

The negative values of  $\Delta G$  for Pb sorption showed that the adsorption process was feasible and spontaneous while the positive  $\Delta G$  values for Cu, Cr and Ni sorption is an indication that the adsorption process was not spontaneous. It has been suggested that positive values for  $\Delta G$  are quite common with ion-exchange mechanism of adsorption of metal ions because of the activated complex of the metal ion formed with the adsorbent in the excited state (Unuabonah et al. 2007). The negative values of  $\Delta G$  for Pb could be associated to the fact that the Pb may have been covalently bound to the surfaces of the adsorbent by complexation mechanisms. Thus, adsorption of Cu, Ni and Cr could also be by ion-exchange mechanism while Pb adsorption could be surface complexation.

## CONCLUSION

This study has investigated the kinetics, isotherm and thermodynamic properties of raw kaolinite clay for the adsorption of heavy metals (Cu, Cr, Ni and Pb) from their aqueous medium. Findings from this study showed that there is a possible chemical reaction between the adsorbates and adsorbent during the sorption processes as the adsorption equilibrium kinetics correlated reasonably well with the pseudo-second-order model. Freundlich, Langmuir and Elovich isotherms showed the processes to which the metals were adsorbed on the raw clay. Nature of the adsorption processes

as shown by the thermodynamic properties showed that Pb adsorption on the raw clay was endothermic, while Cu, Cr and Ni sorption was exothermic. Also, the adsorption of Pb on the raw clay was spontaneous, while Cu, Cr and Ni sorption on the raw clay was not spontaneous. The result is further supported by the fitness of the Pb, Cr, Ni and Cu to the pseudo-second-order kinetics.

## REFERENCES

- Achmed, A., Kassim J., Suan, T.K., Amat, C. and Seey, T.L. 2012. Equilibrium, kinetic and thermodynamic studies on the adsorption of direct dye unto a novel green adsorbent developed from Ucariagambir extract. *J. Physical Sci.*, 23(1): 1-13.
- Adekeye, D.K., Asaolu, S.S., Adefemi, S.O. and Ibigbami O.A. 2019. Heavy metal adsorption properties of the basement complex of clay deposit in Ire-Ekiti Southwestern Nigeria. *IOSR J. Environ. Sci. Toxicol. Food Tech.*, 13(2):1-8.
- Akpomie, K.G., Odewole, O.A., Ibeji, C.U., Okagu, O.D. and Agboola, I.I. 2017. Enhanced sorption of trivalent chromium unto novel cassava peel modified kaolinite clay. *Der. Pharma. Chemica.*, 9(5): 48-55.
- Arnawong, S., Suksabye, P. and Thiravetyan, P. 2016. Using Kaolin in reduction of arsenic in rice grains: Effect of different types of Kaolin, pH and arsenic complex. *Bull. Environ. Contam. Toxicol.*, 96: 556-561.
- Babel, S. and Kurniawan, T.A. 2003. Low-cost adsorbents for heavy metals uptake from contaminated water: a review. *J. Hazard. Materials*, 97(1): 219-243.
- Bailey, S. E., Olin, T. J., Bricka, R. M. and Adrian, D. D. 1999. A review of potentially low-cost sorbents for heavy metals. *Water Research*, 33(11): 2469-2479.
- Barhoumi, S., Messaoudi, I., Deli, T., Said, K. and Kerkeni, A. 2009. Cadmium bioaccumulation in three benthic fish species, *Salaria basilisca*, *Zosterisessor ophiocephalus* and *Solea vulgaris* collected from the Gulf of Gabes in Tunisia. *J. Environ. Sci.*, 21(7): 980-984.
- Brad, H. B. 2004. Adsorption of heavy metal ions on soils and soils constituents. *J. Colloid Interface Sci.*, 277(1): 1-18.
- Dawodu, F. A., Akpomie G. K. and Ejikeme P. C. N. 2012. Equilibrium, thermodynamic and kinetic studies on the adsorption of lead (II) from solution by "Agbani Clay". *Research J. Engine. Sci.*, 1(6): 9-17.

- Eba, F., Gueu, S., Eya' A-Mvongbote A., Ondo J. A., Yao B. K., Ndong N. J., and Kouya, B.R. 2010. Evaluation of the absorption capacity of the natural clay from Bikougou (Gabon) to remove Mn (II) from aqueous solution. *Inter. J. Engine. Sci. Tech.*, 10: 5001-5016.
- El-Sayed G.O., Aly H.M. and Hussien S.H.M. 2011. Removal of acrylic dye blue-5G from aqueous solution by adsorption on activated carbon prepared from maize crops. *Int. J. Res. Chem. Environ.*, 1: 132-140
- El-Sheikh, A.H., Newman, A.P., Al-Daffae, H.K., Phull, S. and Cresswell, N. 2004. Characterization of activated carbon prepared from a single cultivar of Jordanian Olive stones by chemical and physicochemical techniques. *J. Anal. Appl. Pyrolysis*, 71: 151-164.
- Eloussaief, M., Jarraya, I. and Benzina, M. 2009. Adsorption of copper ions on two clays from Tunisia: pH and temperature effects. *Appl. Clay Sci.*, 46(4): 409-413.
- Eloussaief, M. and Benzina, M. 2010. Efficiency of natural and acid activated clays in the removal of Pb(II) from aqueous solutions. *J. Hazard. Mater.*, 178(1-3): 753-757.
- Emam, A.A., Ismail, L.F.M., AbdelKhalek, M.A. and Azza, R. 2016. Adsorption study of some heavy metal ions on modified kaolinite clay. *Intern. J. Advance. Enginee. Tech. Manag. Appl. Sci.*, 3(7): 152-163.
- Freundlich, H.M.F. 1906. Over the adsorption in solution. *J. Phys. Chem.*, 57: 385-471.
- Fu, F. and Wang, Q. 2011. Removal of heavy metal ions from wastewaters: A review. *J. Environ. Manag.*, 92(3): 407-418.
- Garg, K.V., Amita, M., Kumar, R. and Gupta, R. 2004. Basic dye (methylene blue) removal from simulated wastewater by adsorption using Indian Rosewood sawdust: A timber industry waste. *Dyes Pigments*, 63: 243-250.
- Gonzalez, R.J., Videa, P.J.R. Rodriguez, E., Ramirez, S.L., and Gardearres-dey J.L. 2005. Determination of thermodynamics parameters of Cr(VI) adsorption from aqueous solution onto *Agave lechuguilla* biomass. *J. Chem. Thermodynamics*, 37: 343-347.
- Guadalupe, R., Reynel-Avila, H.E., Bonilla-Petriciolet, A. Cano-Rodríguez, I., Velasco-Santos, C. and Martínez-Hernández, A.L. 2008. Recycling poultry feathers for Pb removal from wastewater: Kinetic and equilibrium studies. *Proceedings of World Academy of Science, Engineering and Technology*, 30.
- Ho, Y.S. and McKay, G. 1999. Pseudo-second order model for sorption process. *Process Biochem.*, 34(5): 451-465.
- Kinniburgh, D.G. 1986. General purpose adsorption isotherms. *Environ. Sci. Tech.*, 20(9): 895-904.
- Ku, Y. and Jung, I.L. 2001. Photocatalytic reduction of Cr(VI) in aqueous solutions by UV irradiation with the presence of titanium dioxide. *Water Research*, 35(1): 135-142.
- Kumara, P. S., Ramalingamb, S., Kiruphac, S. D., Murugesan, A. Vidhyadevic, T. and Sivanesan, S. 2011. Adsorption behavior of nickel(II) onto cashew nut shell: Equilibrium, thermodynamics, kinetics, mechanism and process design. *Chemical Engine. J.*, 167: 122-131.
- Lagergren, S. 1908. Zurtheorie der sogenanntes adsorption gelösterstoffe (About the theory of so-called adsorption of soluble substances). *Kungliga Svenska Vetenskapsakademiens. Handlingar*, 24(4): 1-39.
- Langmuir, I. 1918. The adsorption of gases on plane surfaces of glass, mica and platinum. *J. American Chem. Soc.*, 40: 1362-1403.
- Mbaye, A., Diop, C. A., MiehreBrendle, K., Jocelyne, S. F and Maury. T. 2014. Characterization of natural and chemically modified kaolinite from Mako (Senegal) to remove lead from aqueous solutions. *Clay Minerals*, 49: 527-539.
- Mohan, S. and Karthikeyan. J. 1997. Removal of lignin and tannin color from aqueous solution by adsorption on to activated carbon solution by adsorption on to activated charcoal. *Environ. Pollu.*, 97: 183-187.
- Mohan, S.V., Kisa, T., Ohkuma, T., Kanaly, R.A. and Shimizy, Y. 2006. Bioremediation technologies for treatment of PAH-contaminated soil and strategies to enhance process efficiency. *Rev. Environ. Sci. Biotech.*, 5: 347-374.
- Natalia, C. D., Patrícia, A.S. and Maria-Cristina, B. B. 2015. Characterization and modification of a clay mineral used in adsorption tests. *J. Mineral Mater. Characteriz. Engine.* 3: 277-288.
- Nethaji, A., Sivasamy, A. and Mandal, B. 2013. Adsorption isotherms, kinetics and mechanism for the adsorption of cationic and anionic dyes onto carbonaceous particles prepared from *Juglansregia* shell biomass. *Int. J. Environ. Sci. Technol.*, 10: 231-242.
- Olivella, M.A., Jove, P. and Oliveras, A. 2011. The use of cork waste as a biosorbent for persistent organic pollutants—study of adsorption/desorption of polycyclic aromatic hydrocarbons. *J. Environ. Sci. Health A Tox. Hazard. Subst. Environ. Eng.*, 46: 824-832.
- Olu-Owolabi, B.I., Alabi, A.H., Unuabonah, E.I., Diagboya, P.N., Böhm, L. and During, R. 2016. Calcined biomass-modified bentonite clay for removal of aqueous metal ions. *J. Environ. Chem. Enginee.*, 4: 1376-1382.
- Petit, S., Decarreau, A., Mosser, C., Ehret, G. and Grauby, O. 1995. Hydrothermal synthesis (250°C) of copper substituted kaolinites. *Clay Minerals*, 43: 482-494.
- Ramesh, A., Lee, D.J. and Wong, J.W.C. 2005. Thermodynamic parameters for adsorption equilibrium of heavy metals and dyes from wastewater with low-cost adsorbents. *J. Colloid Interface Sci.*, 291: 588-592.
- Rattanaphani, S., Chairat, M., Bremner, J. and Rattanaphani, V. 2007. An adsorption and thermodynamics study of lac dyeing on cotton pretreated with chitosan. *Dyes and Pigment*, 72: 88-96.
- Rengaraj, S., Moona, S.H., Sivabalan, R., Arabindoo, B. and Murugesan, V. 2002. Removal of phenol from aqueous solution and resin manufacturing industry wastewater using an agricultural waste: Rubber seed coat. *J. Hazard Mater.*, 89: 185-196.
- Saikia, N.J., Bharali, D.J., Sengupta, P., Bordoloi D., Goswamee, R.L., Saskia, P.C. and Borthakur, P.C. 2003. Characterization, beneficiation and utilization of a kaolinite clay from Assam, India. *Applied Clay Science*, 24: 93-103.
- Senthilkumar, S., Varadarajan, P.R., Porkodi, P.K. and Subbhuraam, C.V. 2005. Adsorption of methylene blue onto jute fiber carbon: kinetics and equilibrium studies. *J. Colloid Interface Sci.*, 284: 78-82.
- Shawabke, R.A., Rockstraw, D.A. and Bhada, R.K. 2002. Copper and strontium adsorption by a novel carbon material manufactured from pecan shells. *Carbon*, 40: 781-786.
- Shim, H.Y., Lee, K.S., Lee, D.S. and Jeon, D.S. 2014. Application of electrocoagulation and electrolysis on the precipitation of heavy metals and particulate solids in washwater from the soil washing. *J. Agric. Chem. Environ.*, 3(4): 130-138.
- Tsenga, R.L., Wub, F.C. and Juang, R.S. 2003. Liquid-phase adsorption of dyes and phenols using pinewood-based activated carbons. *Carbon*, 41: 487-495.
- Unuabonah, E.I., Adebowale, K.O. and Olu-Owolabi, B.I. 2007. Kinetic and thermodynamic studies of the adsorption of lead (II) ions onto phosphate modified kaolinite clay. *J. Hazard. Mater.*, 144: 386-395.
- Voudrias, E., Fytianos, F. and Bozani, E. 2002. Sorption description isotherms of Dyes from aqueous solutions and wastewaters with different sorbent materials, *Global Nest. Int. J.* 4(1): 75-83.
- Pham, T.D., Nguyen, H.H., Nguyen, N.V., Vu, T.T., Pham, T.N.M., Doan, T.H.Y., Nguyen, M.H. and Ngo, T.M.V. 2017. Adsorptive removal of copper by using surfactant modified laterite soil. *Journal of Chemistry, Article ID 1986071*, 1-11.
- Van der-Marel, H.W. and Beutelspacher, S. 1976. *Atlas of Infrared Spectroscopy of Clay Minerals and Their Mixtures*. Elsevier, Amsterdam, pp. 397.
- Wilson, M.J. 1994. *Clay Mineralogy: Spectroscopic and Chemical Determinative Methods*, Chapman and Hall, London, UK18-60.
- Zouraihi, M., Ammuri, A. K. Z. and Saidi, M. 2016. Adsorption of Cu(II) onto natural clay: Equilibrium and thermodynamic studies. *J. Mater. Environ. Sci.*, 7(2): 566-570.